SCIENTIFIC REPORTS

OPEN

Strengthen of magnetic anisotropy of Au/Co/Au nanostructure by surface plasmon resonance

Received: 2 January 2019
Accepted: 29 May 2019
Published online: 14 June 2019

Yusuke Kikuchi[1,2] & Takuo Tanaka[1,2,3]

We experimentally demonstrated the increase of in-plane magnetic anisotropy in Au/Co/Au nanostructures by localized surface plasmon resonance (LSPR). When an array of Au/Co/Au square patch nanostructures was illuminated with linearly polarized light whose wavelength was 750 nm, the localized surface plasmons were resonantly excited in the nanostructures. From the measurement results of polar magneto-optical Kerr effect curves, we observed the magnetic anisotropy field increase in the Au/Co/Au nanostructure due to the excited surface plasmons. The in-plane magnetic anisotropy energy density was increased about 24%.

Magnetic properties of magnetic devices strongly depend on their materials, the fabrication process, and the surrounding environments. When we want to modulate the magnetization properties of these devices after they have been made, external stimuli such as heat, pressure, and so on, are applied[1–3]. To develop ultra-fast magnetic memory devices, several magnetization control techniques have been proposed, including the voltage-driven magnetization switching[4–6], photo-induced magnetization[7–9], and helicity-dependent magnetic switching[10–12]. However, these phenomena are only observed under the limited conditions like using ultrathin magnetic film with a thickness below 1 nm[4–6], in ultra-low temperature[7–9], or using a femtosecond pulsed laser irradiation[10–12]. Recently, several groups have reported that the magneto-optical effect is enhanced at the resonant wavelength of the localized surface plasmons (LSPs) in metal nanostructures at room temperature[13–17]. This research field is now called as "magneto-plasmonics[18–20]". Our group also has reported that the longitudinal magneto-optical Kerr effect and magneto-optical figure of merit in Au/Co/Au nanostructure is enhanced by the localized surface plasmons excitation[21]. According to these reports, the LSPs affect (and modulate) on the magneto-optical property of the magnetic thin film, but it still remains undiscussed whether the surface plasmon excitation affects the magnetization mechanism or not.

Magnetic anisotropy is an essential factor for practical applications, because it determines the thermal stability of magnetic devices, like magnetic random access memory (MRAM) and magnetic recording devices (e.g. hard disk drive), just to name a few[22,23]. In these devices, the magnetic anisotropy usually decreases when the temperature of the material increases. Heat-assisted magnetic recording (HAMR) technology exploits this phenomenon by modulating the magnetic anisotropy through temporary heating of the recording media and then writing tiny (high-density) data bits on the media[24,25]. In this paper, we report the first demonstration of the increase of the in-plane magnetic anisotropy in Au/Co/Au nanostructure under the LSPR and we also discussed its mechanism.

Methods

Figure 1(a) shows the schematic of the fabricated nanostructure including a cross section of the thin film's stacking order. An array of these square patch nanostructures (170 nm × 170 nm in lateral direction) consisting of Cr (5 nm)/Au (30 nm)/Co (6 nm)/Au (30 nm) were fabricated on an ITO substrate using electron beam lithography. The Cr layer serving as an adhesive layer for Au, was initially deposited by thermal evaporation. The succeeding Au, Co, and again Au layers were continuously deposited using electron beam evaporation right after thermal evaporation in the same chamber and the same vacuum condition. Finally, after the liftoff process, Au/Co/Au nano square patch array was obtained. Figure 1(b) is the scanning electron microscope (SEM) image of the fabricated nanostructures. The distance between the center of each square in the x and y directions is 480 nm. The optical properties of the

[1]School of Materials and Chemical Technology, Tokyo Institute of Technology, 2-12-1 Ookayama, Meguroku, Tokyo, 152-8550, Japan. [2]Metamaterials Laboratory, RIKEN Cluster for Pioneering Research, 2-1 Hirosawa, Wako, Saitama, 351-0198, Japan. [3]Innovative Photon Manipulation Research Team, RIKEN Center for Advanced Photonics, 2-1 Hirosawa, Wako, Saitama, 351-0198, Japan. Correspondence and requests for materials should be addressed to T.T. (email: t-tanaka@riken.jp)

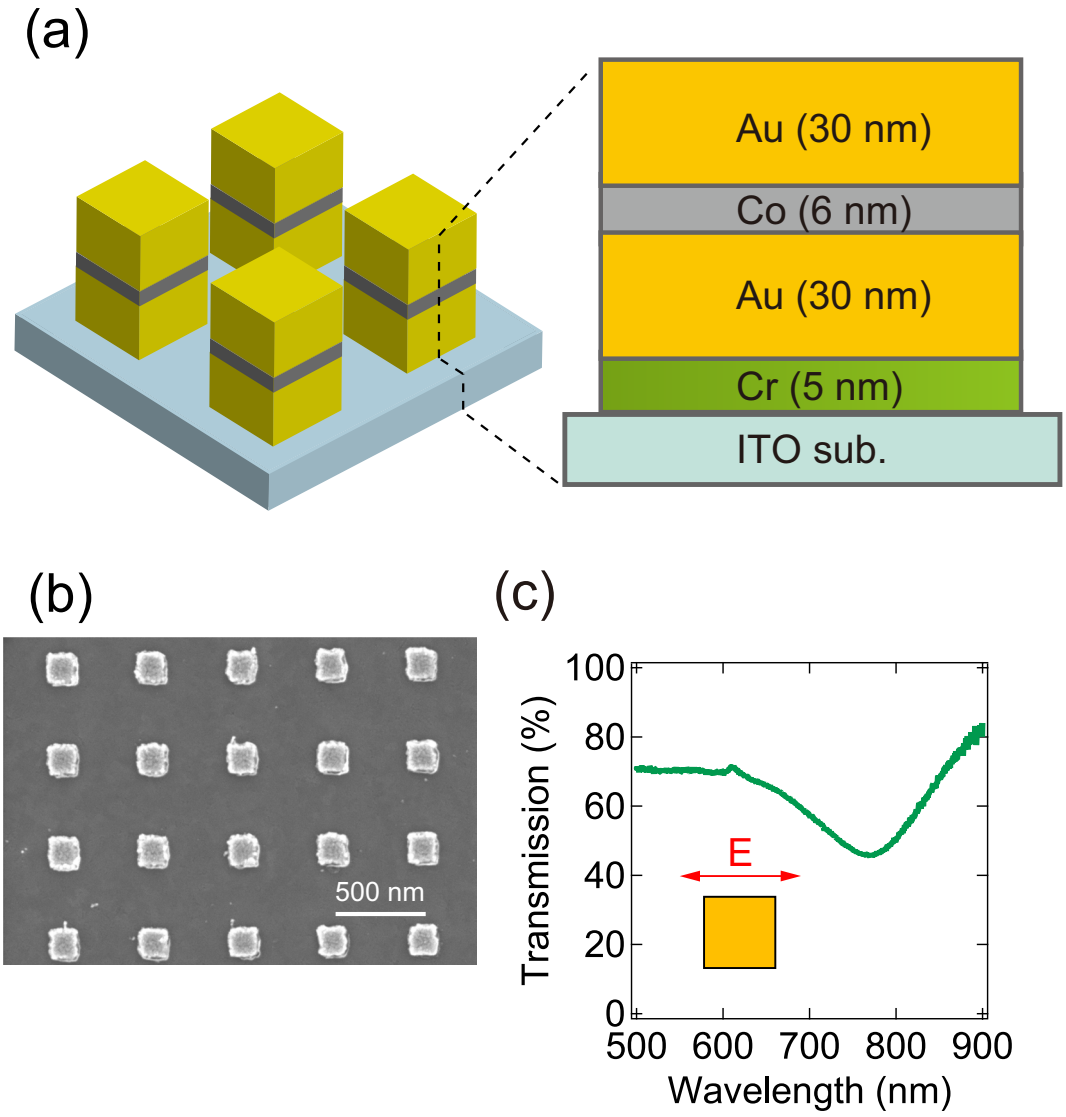

Figure 1. (**a**) Schematic of the fabricated nanostructure and the stacking structure of the thin film (cross-section view). (**b**) SEM image of fabricated Au/Co/Au nanostructures. (**c**) Transmission spectra of Au/Co/Au nanostructure.

sample were characterized by measuring transmission spectra using a UV-visible spectrometer (Ocean Optics, USB2000 + XR1-ES). The characteristics of the sample structure's magnetic anisotropy at room temperature were evaluated by the magnetic field dependence of the longitudinal and the polar magneto-optical Kerr effects since the magneto-optical Kerr effect reflects the magnetization of materials[26]. The in-plane magnetization curve was evaluated by a longitudinal magneto-optical Kerr effect (L-MOKE) measurement system based on a polarization modulation technique using a photoelastic modulator (PEM)[26,27]. In this experiment, diode lasers with wavelengths of v640 and 785 nm were used as light sources and these laser beams were introduced onto the sample surface at a fixed incident angle of 14° and their polarization were set parallel to the edge of the nanostructure surface. The incident laser intensity was set to 142 mW/mm^2. The magnetic field of 1000 Gauss was applied parallel to the sample surface.

The out-of-plane magnetization curve was evaluated via a polar magneto-optical Kerr effect (P-MOKE) measurement system (MODEL BH-M800UV-HD-10, NEOARK CORP.). In this system, a xenon lamp was used as a light source, and the wavelength (λ) of the incident light was selected by a monochromator. The plane of incidence was set parallel to the edge of the nanostructure surface. The incident angle was fixed at about 5°. The incident light intensity in P-MOKE measurement is estimated to be less than 1.4 $\mu W/mm^2$. A magnetic field of ±20 k Gauss was applied perpendicular to the sample plane.

Results

First of all, in order to evaluate the plasmonic properties of the fabricated Au/Co/Au nanostructure, we measured the transmission spectra as shown in Fig. 1(c). The polarization direction of the incident light was parallel to the edge of nano square patch as the inset of Fig. (c). From this result, we confirmed that the absorption peak originating from the SPR was observed only at $\lambda = 770$ nm, and no other absorption peaks were found in the

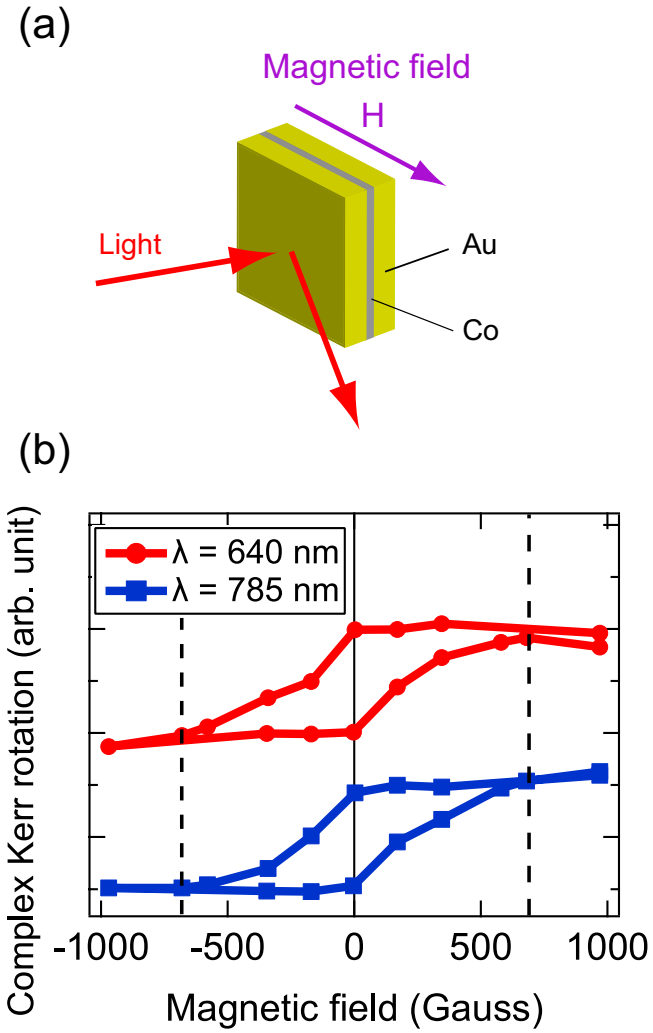

Figure 2. (**a**) Longitudinal magneto-optical Kerr effect (L-MOKE) measurement configuration. Magnetic field (H) is applied parallel to the surface of the Au/Co/Au nanostructure. (**b**) Magnetic field dependence of normalized complex Kerr rotation in longitudinal configuration (L-MOKE curve) for Au/Co/Au nanostructure at two different incident wavelengths (λ): 640 nm – off-resonance (red circles and line) and 785 nm – on-resonance (blue squares and line).

range of $\lambda = 500$ to 640 nm. This result indicates that LSPs excitation can be switched on and off by changing the wavelength of the incident light and this is why we chose light sources whose wavelength are close to 770 nm in the L-MOKE and P-MOKE experiments to induce LSPR.

Figure 2 shows the relationship between the applied magnetic field and the complex longitudinal Kerr rotation (L-MOKE curve). Clear hysteresis loops of the L-MOKE curves were obtained for both $\lambda = 640$ nm (red circles, off-resonance) and 785 nm (blue squares, on-resonance). In addition, there is no significant difference of the saturation field even by changing the wavelength of the incident light.

Figure 3 shows the relationship between the normalized Kerr ellipticity (η) and the external magnetic field in polar geometry (P-MOKE curve) measured with $\lambda = 500$ and 750 nm. As shown in Fig. 3(a), P-MOKE curves for both $\lambda = 500$ nm (red line, off-resonance) and 750 nm (blue line, on-resonance) do not exhibit any hysteresis loops unlike the L-MOKE curves. However, the saturated magnetization field, indicated by black arrows, in P-MOKE curves is about 10 times stronger than that of L-MOKE curves. These results imply that (1) Au/Co/Au nanostructure has a magnetic anisotropy and (2) the easy magnetization axis is parallel to the film plane. In addition, we found that there was a significant difference between the shape of P-MOKE curves for $\lambda = 500$ and 750 nm. To clarify this difference, we estimated the slope of the P-MOKE curve ($\Delta\eta/\Delta H$) in the range from −6 k to 6 k Gauss for $\lambda = 500$ and 750 nm to be 0.148 and 0.120 (unit: arb. unit of Kerr ellipticity/k Gauss), respectively. We evaluated the magnetic anisotropy field (H_k) in the P-MOKE curve. H_k is defined as the intersection of the fitted line of $\Delta\eta/\Delta H$ ($\lambda = 500$ nm, red dashed line; $\lambda = 750$ nm, blue dashed line) and the fitted line of the saturation Kerr ellipticity (black dashed line) in the range of −13 k to −20 k and 13 k to 20 k Gauss (Fig. 3(b)). The average magnitude of H_k in $\lambda = 500$ and 750 nm were about 7.10 k and 9.03 k Gauss, respectively. Reflection

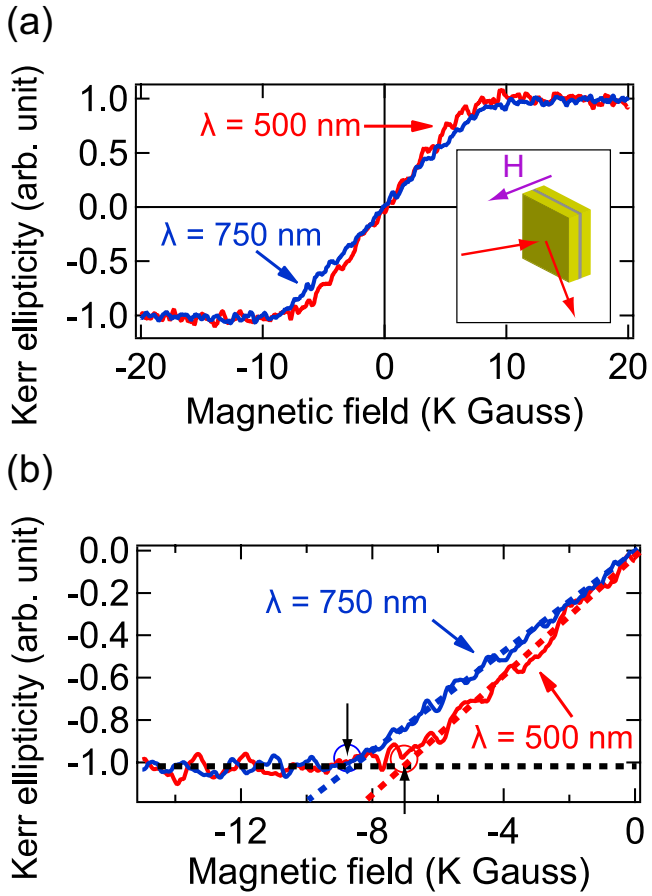

Figure 3. (**a**) Magnetic field dependence of normalized Kerr ellipticity in polar configuration (P-MOKE curve) for Au/Co/Au nanostructure at two different incident wavelengths (λ): 500 nm (red line) and 750 nm (blue line). The insert is schematic of polar magneto-optical Kerr effect (P-MOKE) measurement configuration. Magnetic field (H) is applied perpendicular to the surface of the Au/Co/Au nanostructure. (**b**) P-MOKE curves of Au/Co/Au nanostructure at the negative magnetic field region. Red dashed lines is the fitted data for 500 nm and blue dashed lines is for 750 nm. Black dashed line is the saturation of Kerr ellipticity. The intersection of the black dashed line and the red or the blue dashed lines gives the saturation magnetic field. Black arrows indicate the saturation magnetic fields for λ = 500 nm (red circle) and 750 nm (blue circle).

on some of these results made clear that H_k was drastically increased when the surface plasmons were excited in the structure ($\lambda = 750$ nm).

In order to investigate the wavelength dependence of H_k in a Co thin film and compare with that of Au/Co/Au structure, we fabricated a bare 20 nm-thick Co thin film and measured its H_k at different wavelengths of irradiated light. The fabrication process of Co thin film is the same as that of the Au/Co/Au nanostructure. Figure 4(a) shows the transmittance spectrum of the Co thin film. No absorption peak was observed in the visible to near infrared region. This indicates LSPs were not excited in the bare Co thin film at the given wavelength region. Figure 4(b) shows the L-MOKE curve of the Co thin film for $\lambda = 785$ nm, and it presents clear hysteresis characteristics to the applied magnetic field. Figure 4(c) shows the P-MOKE curves of the Co thin film for $\lambda = 500$ nm and 750 nm. The overlapping of these two P-MOKE curves indicates that there is no wavelength dependence of H_k in the Co thin film. Therefore, we concluded that the remarkable increment of H_k in the Au/Co/Au nanostructure originated from the LSPs excited on Au.

Discussion

From the magnetization curve, the in-plane magnetic anisotropy energy density (K_u) in a thin film can be calculated as follows,

$$K_u = \left(\int H_{\perp} dM\right) - \left(\int H_{//} dM\right), \quad (1)$$

where M are magnetization and, $H_{\perp}$ and $H_{//}$ are magnetic field applied perpendicular and parallel to the surface of thin film, respectively. Using both L-MOKE and P-MOKE curves along with Eq. (1), we calculated the in-plane magnetic anisotropy energy density in the Au/Co/Au nanostructure with LSPs ($K_{u,wLSPs}$) and without LSPs ($K_{u,w/oLSPs}$),

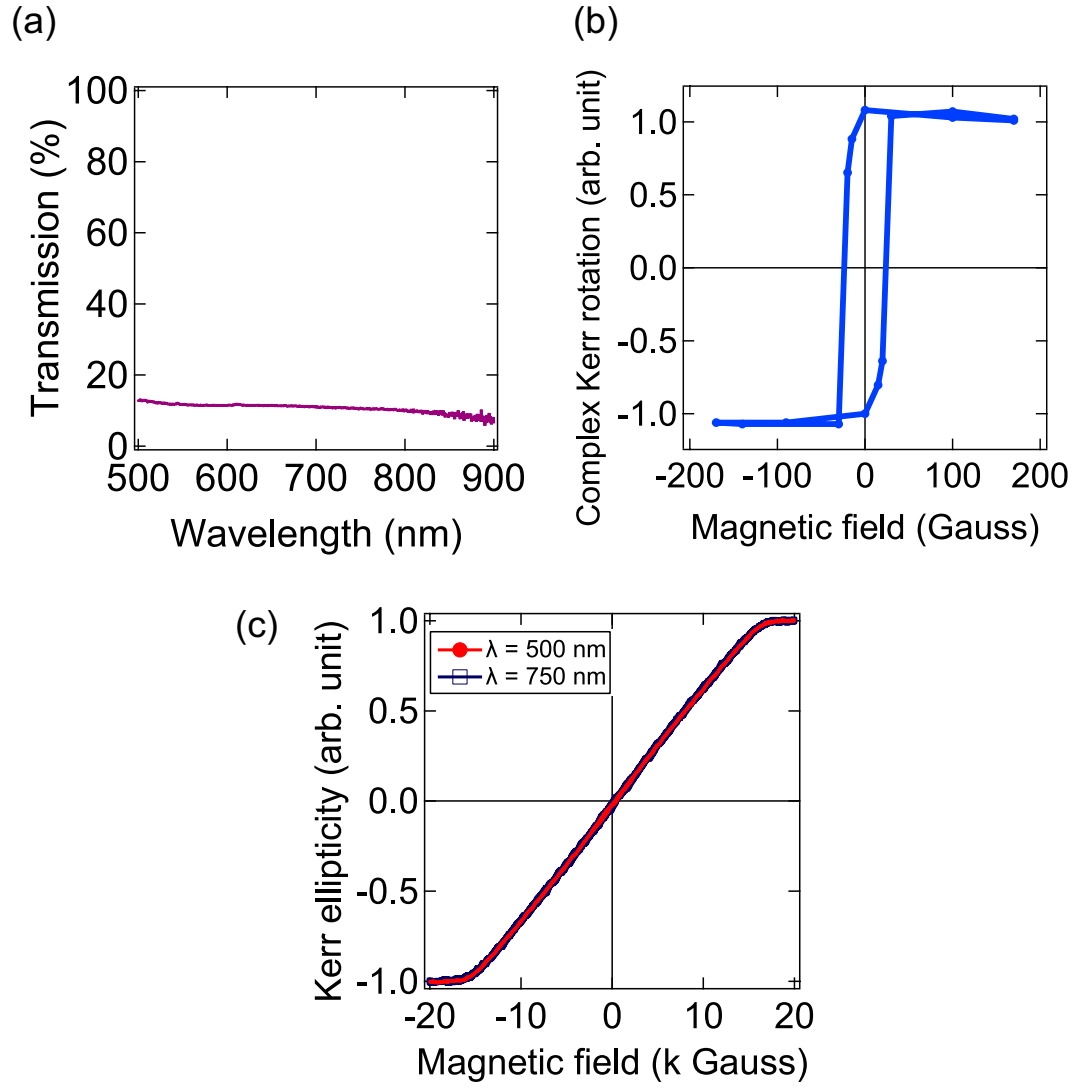

Figure 4. (**a**) Transmission spectrum of 20 nm-thick Co thin film. (**b**) Magnetic field dependence of normalized complex Kerr rotation in longitudinal configuration (L-MOKE curve) for 20 nm-thick Co thin film. (**c**) Magnetic field dependence of normalized Kerr ellipticity in polar configuration (P-MOKE curve) for the Co thin film with two different incident wavelengths (λ): 500 nm (red circles and line) and 750 nm (blue hollow squares and line).

assuming a linear relationship between Kerr ellipticity (or complex Kerr rotation) and magnetization. The equations are as follows:

$$K_{\mathrm{u,wLSPs}} = \frac{M_s}{\eta_s}\left(\int_0^{\eta_s} H_{\perp} d\eta_k\right)^{\lambda=750\ nm} - \frac{M_s}{\Phi_s}\left(\int_0^{\Phi_s} H_{//} d\Phi_k\right)^{\lambda=785\ nm}, \tag{2}$$

$$K_{\mathrm{u,w/oLSPs}} = \frac{M_s}{\eta_s}\left(\int_0^{\eta_s} H_{\perp} d\eta_k\right)^{\lambda=500\ nm} - \frac{M_s}{\Phi_s}\left(\int_0^{\Phi_s} H_{//} d\Phi_k\right)^{\lambda=640\ nm}, \tag{3}$$

where M_s, η_s, η_k, Φ_s, and Φ_k are saturated value of magnetization, saturated Kerr ellipticity, Kerr ellipticity, saturated complex Kerr rotation, and complex Kerr rotation, respectively. $M_s = 900$ emu/cm^3 was used for 6 nm-thick Co thin film based on ref.[28]. Using Eqs (2) and (3), $K_{\mathrm{u,wLSPs}}$ and $K_{\mathrm{u,w/oLSPs}}$ were calculated as 0.383×10^6 J/m^3 and 0.310×10^6 J/m^3, respectively. This result implies that the in-plane magnetic anisotropy energy increases when LSPs are excited.

In a thin film, its magnetic anisotropy consists of both magnetocrystalline anisotropy and shape anisotropy[29,30]. In our case, the magnetic anisotropy energy modulation would come from the change of magnetocrystalline anisotropy because we used the same sample in all experiments and we verified that there was no sample deformation through all experiments.

To understand the results, we would like to discuss about the thermal effect on the magnetic anisotropy due to temperature increase from plasmon induced light absorption[31]. There are many theoretical and experimental works on the temperature dependence of magnetocrystalline anisotropy energy[32–34]. In all these works, decrease in the magnetocrystalline anisotropy energy has been observed with an increase of temperature. Our results, on the other hand, are different from these, because we observed that in-plane magnetocrystalline anisotropy energy increases as temperature increases. Here, we present possible scenarios to explain our results.

As stated above, the total in-plane magnetic anisotropy energy K_u, which can be estimated from a magnetization loops shown in Figs 3 and 4(c), is written as a sum of shape anisotropy K_s, which comes from magnetostatic property, and a magnetocrystalline anisotropy K_i as below,

$$K_u = K_s + K_i. \tag{4}$$

In the case of thin film structure, whose thickness is thinner than its lateral dimension, the easy magnetization direction is parallel to the film surface and K_s has positive value. However, the size of structure becomes nanometer scale, the estimation and calculation of K_s is difficult and unreliable, because (1) the magnetization distribution in the nanostructure is complicated[35] and (2) the magnetization of magnetic nanostructure cannot be measured directly. According to ref.[35], magnetization vector in the square nanostructure are easily aligned to the in-plane direction and what we can say is K_s has positive value. Meanwhile, about K_i, we can obtain its value neither by measuring nor calculation. Hence, it is possible to build up two hypotheses. One is K_i has negative value and another is it has positive value.

When we assumed that the sign of K_i is negative, which means the magnetization of nanostructure is perpendicular to the film surface, K_i reduces K_u and K_s should be larger than $|K_i|$ because K_u was positive which has already confirmed above using the L-MOKE and P-MOKE loops. Under this condition, when the temperature of the structure increases due to the plasmon resonance, K_i approaches zero and, as a result, K_u increases effectively. A similar phenomenon has been observed and reported in the magnetic thin film but never in nanostructures[36].

Another possibility is the sign of K_i is positive, which is the same to that of Au/Co/Au thin film shown in Supplementary Information. When K_i has a positive value and decreases with the temperature increase by LSP excitation, K_u also always decreases. In this case, to explain our results showing an overall K_u increase by LSP resonance plausibly, it is necessary to introduce a new term K_p, which is the plasmon-induced in-plane magnetic anisotropy energy. Moreover, even if the K_i decreases with increasing the temperature by LSP excitation, K_p increases K_u more than the decrease of K_i. Finally, we propose a possible origin of plasmon-induced in-plane magnetic anisotropy. When LSPs are resonantly excited by light in metal nanostructure, collective electron oscillations are induced by the electric field of the incident light, which means that electric polarization is induced in the metal nanostructure by LSP excitation[37]. According to ref.[38], by using a ferromagnetic insulator, they derived an expression to describe the electric polarization ($\overrightarrow{P}$) dependence of magnetocrystalline anisotropy energy (K_i) as

$$K'_i = K_i + \left(\frac{\partial K'_i}{\partial \overrightarrow{P}}\right)_0 \cdot \overrightarrow{P}, \tag{5}$$

where K'_i is the $\overrightarrow{P}$-dependent K_i. Therefore, magnetocrystalline anisotropy energy increase via LSP resonance-induced electric polarization may be essential for the overall K_u increase by LSP resonance.

In summary, the increase of magnetic anisotropy energy in Au/Co/Au nanostructure was initially observed experimentally under the localized surface plasmon resonance. The increase of in-plane magnetic anisotropy energy density was estimated to be $0.73 \times 10^5\,J/m^3$. We suggest that the increase of the magnetic anisotropy energy originates from the alteration of magnetocrystalline anisotropy by LSPs excitation.

References

1. Onose, Y., Takeshita, N., Terakura, C., Takagi, H. & Tokura, Y. Doping dependence of transport properties in $Fe_{1-x}Co_xSi$. *Physical Review B* **72**, 224431 (2005).
2. Matsushita, M., Endo, S., Miura, K. & Ono, F. Pressure-induced change of the magnetic state in ordered Fe–Pt Invar alloy. *Journal of Magnetism and Magnetic Materials* **269**, 393 (2004).
3. Iwamoto, T., Mito, M., Hidaka, M., Kawase, T. & Takeda, K. Magnetic measurement of rare earth ferromagnet gadolinium under high pressure. *Physica B* **329**, 667 (2003).
4. Hsu, P.-J. *et al*. Electric-field-driven switching of individual magnetic skyrmions. *Nature Nanotechnology* **12**, 123 (2017).
5. Kikuchi, Y., Seki, T., Kohda, M., Nitta, J. & Takanashi, K. Voltage-induced coercivity change in FePt/MgO stacks with different FePt thicknesses. *Journal of Physics D-Applied Physics* **46**, 285002 (2013).
6. Maruyama, T. *et al*. Large voltage-induced magnetic anisotropy change in a few atomic layers of iron. *Nature nanotechnology* **4**, 158 (2009).
7. Ohkoshi, S., Imoto, K., Tsunobuchi, Y., Takano, S. & Tokoro, H. Light-induced spin-crossover magnet. *Nature chemistry* **3**, 564 (2011).
8. Brinzari, T. V. *et al*. Light-induced magnetization changes in aggregated and isolated cobalt ferrite nanoparticles. *Journal of Applied Physics* **124**, 103904 (2018).
9. Pinkowicz, D. *et al*. Enforcing Multifunctionality: A Pressure-Induced Spin-Crossover Photomagnet. *Journal of the American chemical society* **137**, 8795 (2015).
10. Kimel, A. V., Kirilyuk, A. & Rasing, T. Femtosecond opto-magnetism: ultrafast laser manipulation of magnetic materials. *Laser & Photonics Reviews* **1**, 275 (2007).
11. Mangin, S. *et al*. Engineered materials for all-optical helicity-dependent magnetic switching. *Nature materials* **13**, 286 (2014).
12. Lambert, C.-H. *et al*. All-optical control of ferromagnetic thin films and nanostructures. *Science* **345**, 1337 (2014).
13. Meneses-Rodriguez, D. *et al*. Probing the Electromagnetic Field Distribution within a Metallic Nanodisk. *Small* **7**, 3317 (2011).
14. Maccaferri, N. *et al*. Tuning the Magneto-Optical Response of Nanosize Ferromagnetic Ni Disks Using the Phase of Localized Plasmons. *Physical Review Letters* **111**, 167401 (2013).

15. Yamane, H., Takeda, K. & Kobayashi, M. Magneto-plasmonics on perpendicular magnetic CoPt–Ag nanostructures with ZnO intermediate thin layers. *Applied Physics Letters* **106**, 052409 (2015).
16. Herreño-Fierro, C. A., Patiño, E. J., Armelles, G. & Cebollada, A. Surface sensitivity of optical and magneto-optical and ellipsometric properties in magnetoplasmonic nanodisks. *Applied Physics Letters* **108**, 021109 (2016).
17. Choi, B. C., Xu, H., Hajisalem, G. & Gordon, R. Localized surface plasmon resonance enhanced magneto-optical Kerr effect in $Ni_{80}Fe_{20}$ thin films coated with Au nanorods. *Applied Physics Letters* **112**, 022403 (2018).
18. Armelles, G., Cebollada, A., Garcia-Martin, A. & Gonzalez, M. U. Magnetoplasmonics: Combining Magnetic and Plasmonic Functionalities. *Advanced Optical Materials* **1**, 10 (2013).
19. Sander, D. *et al*. The 2017 Magnetism Roadmap. *Journal of Physics D-Applied Physics* **50**, 33 (2017).
20. Kuzmin, D. A., Bychkov, I. V., Shavrov, V. G. & Temnov, V. V. Plasmonics of magnetic and topological graphene-based nanostructures. *Nanophotonics* **7**, 597 (2018).
21. Kikuchi, Y. & Tanaka, T. Plasmon assisted improvement of figure of merit of magneto-optical Kerr effect in Au/Co/Au multilayered nanorectangular patch array. *Japanese Journal of Applied Physics* **57**, 110305 (2018).
22. Wu, X. W., Guslienko, K. Y., Chantrell, R. W. & Weller, D. Magnetic anisotropy and thermal stability study on FePt nanoparticle assembly. *Applied Physics Letters* **82**, 3475 (2003).
23. Kim, G., Sakuraba, Y., Oogane, M., Ando, Y. & Miyazaki, T. Tunneling magnetoresistance of magnetic tunnel junctions using perpendicular magnetization $L1_0$ -CoPt electrodes. *Applied Physics Letters* **92**, 172502 (2008).
24. Challener, W. A. *et al*. Light Delivery Techniques for Heat-Assisted Magnetic Recording. *Japanese Journal of Applied Physics* **42**, 981 (2003).
25. Zavaliche, F. *et al*. Electrically Assisted Magnetic Recording in Multiferroic Nanostructures. *Nano Letters* **7**, 1586 (2007).
26. Sato, K. *et al*. Magnetooptical Kerr Spectrometer for 1.2-5.9 eV Region and its Application to FePt/Pt Multilayers. *Japanese Journal of Applied Physics Part 1-Regular Papers Short Notes & Review Papers* **32**, 989 (1993).
27. Sato, K. Measurement of Magneto-Optical Kerr Effect Using Piezo-Birefringent Modulator. *Japanese Journal of Applied Physics* **20**, 2403 (1981).
28. Chuang, T. C., Su, P. L., Wu, P. H. & Huang, S. Y. Enhancement of the anomalous Nernst effect in ferromagnetic thin films. *Physical Review B* **96**, 174406 (2017).
29. Weller, D. *et al*. Microscopic Origin of Magnetic Anisotropy in Au/Co/Au Probed with X-Ray Magnetic Circular Dichroism. *Physical Review Letters* **75**, 3752 (1995).
30. Kojima, T. *et al*. Magnetic Anisotropy and Chemical Order of Artificially Synthesized $L1_0$-Ordered FeNi Films on Au–Cu–Ni Buffer Layers. *Japanese Journal of Applied Physics* **51**, 010204 (2012).
31. Baffou, G., Quidant, R. & Girard, C. Heat generation in plasmonic nanostructures: Influence of morphology. *Applied Physics Letters* **94**, 153109 (2009).
32. Zener, C. Classical Theory of the Temperature Dependence of Magnetic Anisotropy Energy. *Physical Review* **96**, 1335 (1954).
33. Melikhov, Y. *et al*. Temperature dependence of magnetic anisotropy in Mn-substituted cobalt ferrite. *Journal of Applied Physics* **99**, 08r102 (2006).
34. Yoon, S. & Krishnan, K. M. Temperature dependence of magnetic anisotropy constant in manganese ferrite nanoparticles at low temperature. *Journal of Applied Physics* **109**, 07b534 (2011).
35. Cowburn, R. P. & Welland, M. E. Phase transitions in planar magnetic nanostructures. *Applied Physics Letters* **72**, 2041 (1998).
36. Berger, A. & Hopster, H. Magnetization reversal properties near the reorientation phase transition of ultrathin Fe/Ag(100) films. *Journal of Applied Physics* **79**, 5619 (1996).
37. Jain, P. K. & El-Sayed, M. A. Plasmonic coupling in noble metal nanostructures. *Chemical Physics Letters* **487**, 153 (2010).
38. Rado, G. T. & Ferrari, J. M. Electric field dependence of the magnetic anisotropy energy in magnetite (Fe_3O_4). *Physical Review B* **12**, 5166 (1975).

Acknowledgements

The authors would like to thank the RIKEN Emergent Matter Science Research Laboratory for the usage of the electron beam lithography and electron beam deposition facility. The authors would also like to thank Akita Industrial Technology Center for the usage of the polar magneto–optical Kerr effect measurement facility. We would like to thank Dr. M.V. Balois for her English correction. Y.K. was financially supported by Junior Research Associate (JRA) program in RIKEN.

Author Contributions

Y.K. carried out the experiments, data analysis and writing of the manuscript. T.T. supervised and coordinated all the work.

Additional Information

Supplementary information accompanies this paper at https://doi.org/10.1038/s41598-019-45122-1.

Competing Interests: The authors declare no competing interests.

Publisher's note: Springer Nature remains neutral with regard to jurisdictional claims in published maps and institutional affiliations.